

## Quarkonia at finite temperature in relativistic heavy-ion collisions

SAUMEN DATTA

Department of Theoretical Physics, Tata Institute of Fundamental Research, Homi Bhabha Road, Mumbai 400 005, India  
E-mail: saumen@theory.tifr.res.in

DOI: 10.1007/s12043-015-0975-y; ePublication: 6 May 2015

**Abstract.** The behaviour of quarkonia in relativistic heavy-ion collisions is reviewed. After a detailed discussion of the current theoretical understanding of quarkonia in a static equilibrated plasma, we discuss quarkonia yield from the fireball created in ultrarelativistic heavy-ion collision experiments. We end with a brief discussion of the experimental results and outlook.

**Keywords.**  $J/\psi$  suppression; quarkonia; quark-gluon plasma.

**PACS Nos** 12.38.Mh; 12.38.Gc; 25.75.Nq

### 1. Introduction

The connection between quarkonia and deconfinement began with the remarkable paper of Matsui and Satz [1]. The basic idea is extremely simple. At high temperatures, due to Debye screening, the binding between a  $\bar{Q}Q$  pair takes the Yukawa form, and for sufficiently high temperatures, the  $\bar{Q}Q$  meson does not form as the binding becomes sufficiently weak. For  $J/\psi$  the temperature was estimated to be very close to  $T_c$ , the temperature for transition from a hadronic state to a deconfined plasma. As  $J/\psi$  shows a prominent peak in the dilepton channel, the disappearance of this peak would be the indicator of deconfinement. In follow-up papers [2,3], the dissociation temperature of various quarkonia was calculated using the Debye screened form. It was found that the 1S charmonia would decay very close to the transition temperature while the 1P, 2S etc. states would decay even earlier. On the other hand, the  $\Upsilon$  was found to survive till much higher temperatures. Therefore, the quarkonia states were suggested as a thermometer for the plasma.

A suppression of the  $J/\psi$  peak was indeed found in the fixed target 158 A GeV Pb–Pb collisions [3a] in the NA50 experiment in CERN [4]. Similar suppression has also been seen in the colliding machine experiments at 200 A GeV Au–Au collision in RHIC, and at 2.76 A TeV Pb–Pb collisions in LHC.

A more detailed theoretical analysis of the behaviour of quarkonia in quark-gluon plasma (QGP), however, has shown more intricacies than originally thought. Even in the case of static equilibrium plasma, theoretically the simplest one to handle, the behaviour of quarkonia seems quite complicated in the temperature regime  $1-3T_c$  which is of interest to relativistic heavy-ion collision experiments. Experimentally, there is strong evidence that a deconfined medium has been formed in relativistic heavy-ion collision experiments. While suppression of quarkonia has been a generic feature in these experiments, the detailed behaviour has been more complicated to understand. Quarkonia remain among the most studied observables in such experiments; but probably they provide an insight into the nature of the plasma rather than act as a thermometer.

Here we shall review our current understanding of the theory of quarkonia in deconfined medium. In the next section, we shall discuss in some detail the idealized problem of quarkonia in an equilibrated plasma at a fixed, not-too-high temperature. In §3, we shall discuss attempts to study quarkonia in the fast expanding fireball that is created in the experiments. Section 4 contains a short outline of the main experimental results, for completeness. The last section contains a summary.

## 2. Quarkonia in static equilibrium plasma

In this section we shall discuss our current theoretical understanding of, and challenges in understanding the behaviour of quarkonia in deconfined plasma. For definiteness, we shall consider the case of a  $\bar{Q}Q$  pair in a definite quantum number channel, put in as probe of the medium, where  $Q$  can be charm or bottom.

As outlined in §1, the first studies of quarkonia in QGP were built on the reasonably successful nonrelativistic potential model approach to quarkonia spectroscopy. Instead of a confining potential, the Debye screened form of the potential,

$$V(r) = -\frac{4}{3} \frac{\alpha_s}{r} e^{-m_D r} \quad (1)$$

was used. Here  $\alpha_s$  is the strong coupling constant and  $m_D$  is the Debye mass in QGP. The aim was to calculate a dissociation temperature for different quarkonia by solving the Schrödinger equation with  $V(r)$ . The perturbative form of the potential was later substituted by the free energy of a static  $\bar{Q}Q$  pair, calculated from the lattice.

Use of eq. (1) in this way, however, is not based on strong theoretical footing. Recent attempts to understand the behaviour of quarkonia in-medium have started with a rephrasing of the question: e.g., “what happens to the  $J/\psi$  peak in the dilepton channel if a plasma is formed?” is best understood by looking at a quantity that directly looks at the dilepton channel.  $J/\psi$  connects to the dilepton channel by the point vector current  $V_i(x) = \bar{c}(x)\gamma_i c(x)$ , and the suitable correlator of this current controls the dilepton rate. The dilepton rate can be directly connected to the spectral function, which is the Fourier transform of the correlator [5],

$$\rho_H(p_0, \vec{p}) = \int dt \int d^3x e^{ip_0 t - i\vec{p}\cdot\vec{x}} \langle [J_H(\vec{x}, t), J_H(\vec{0}, 0)] \rangle, \quad (2)$$

where  $J_H(\vec{x}, t) = \bar{Q}(\vec{x}, t)\gamma_H Q(\vec{x}, t)$  is the suitable hadronic point current, and the angular bracket indicates thermal averaging.  $\rho_H(p_0, \vec{p})$  is called the spectral function and is proportional to the dilepton rate.

A mode expansion of  $\rho_H(p_0, \vec{p})$  is instructive. Inserting a complete set of states, one can write  $\rho_H(p_0, \vec{p})$  as

$$\rho_H(p_0, \vec{p}) = \frac{1}{Z} \sum_{n,m} (e^{-k_n^0/T} - e^{-k_m^0/T}) |\langle n | J_H(0) | m \rangle|^2 \delta^4(p^\mu - k_m^\mu + k_n^\mu), \quad (3)$$

where the sum over states include both discrete and continuous states, and  $k_n^\mu$  is the four-momenta of the state  $|n\rangle$ .

In the case of a free scalar particle of mass  $M$ , this expression leads to a spectral function

$$\rho_H(p_0, \vec{p})|_{\text{free}} = \epsilon(p_0)\delta(p^2 - M^2). \quad (4)$$

As  $T \rightarrow 0$ , a stable meson contributes a similar term to the spectral function in QCD (with a multiplicative factor  $|\langle 0 | J_H | M \rangle|^2$ ). When the state is unstable, the delta function gets smeared into a smooth peak, whose width reflects the decay width of the particle. For a particle like the  $J/\psi$  with a narrow decay width, one gets an almost- $\delta$  function peak, which shows up in the dilepton cross-section. At finite temperatures, as eq. (3) shows, we shall have a more complicated expression; the question of interest is whether the peak structures corresponding to various quarkonia survive at a given temperature.

### 2.1 Spectral function using lattice QCD

QCD, the theory of strong interactions, cannot be directly defined on the continuum (like other quantum field theories), and needs to be regularized. Regularization using a space-time lattice has proved invaluable for studying nonperturbative regime of QCD, as one can use numerical Monte Carlo techniques. Much of our current knowledge of strongly interacting matter at moderately high temperatures (that are of interest to the ultrarelativistic heavy-ion collision experiments), in particular the transition temperature, equation-of-state, nature of the transition, etc., comes from lattice QCD [6].

As we are interested in the spectral function,  $\rho$ , at temperatures  $\lesssim 3T_c$ , where perturbation theory may not work very well, it would be ideal to calculate the spectral function,  $\rho(\omega = p_0, \vec{p})$  using lattice QCD. The catch is that lattice QCD is defined in Euclidean time, and the thermal correlators that one can calculate numerically are the Matsubara correlators

$$C_H(\vec{x}, \tau) = \langle J_H(\vec{x}, \tau) J_H(\vec{0}, 0) \rangle, \quad (5)$$

where  $\tau \in [0, \beta = 1/T)$  is defined in the Euclidean time direction. In order to get the real-time correlators of eq. (2) one needs to use an analytic continuation in time,  $\tau \rightarrow -it$ . This leads to the following integral equation connecting  $\rho_H(\omega, \vec{p})$  and  $C_H(\vec{x}, \tau)$ :

$$C_H(\tau, \vec{p}) = \int d^3x e^{-i\vec{p}\cdot\vec{x}} C_H(\vec{x}, \tau) = \int d\omega \rho_H(\omega, \vec{p}) K(\omega, \tau) \quad (6a)$$

$$K(\omega, \tau) = \frac{\cosh \omega(\tau - 1/2T)}{\sinh \omega/2T}. \quad (6b)$$

For  $T = 0$ , eq. (6a) simplifies to a Laplace transform. In the rest of this section, we shall mostly consider correlators projected to  $\vec{p} = 0$ , and denote them simply as  $C_H(\tau)$ , omitting the  $\vec{p}$  argument. The corresponding spectral function  $\rho_H(\omega, \vec{p} = 0)$  will be written as  $\rho_H(\omega)$ .

The first lattice studies of  $J/\psi$  and other charmonia states are about a decade old [7–9]. They all used the ‘quenched approximation’, i.e., the plasma was purely gluonic.  $\mathcal{O}(10)$  (12-32) data points were used in the  $\tau$  direction, and the spectral function was estimated using eq. (6a). An examination of eq. (6a) immediately shows the difficulty of the extraction of  $\rho_H(\omega)$  from  $C(\tau)$ : the inverse Laplace transform is a very nontrivial problem numerically, made even more difficult by the dual facts of the small range of  $\tau$  at high temperatures and the  $\mathcal{O}(10)$  data points. Note that because of the periodicity of the kernel in eq. (6b), one has independent information about Matsubara correlation only for  $\tau \in [0, \beta/2)$ . Clearly, a direct inversion of eq. (6) is not possible. The studies used the maximum entropy method (MEM) [10], where Bayesian theory is used to provide information about the solution  $\rho_H(\omega)$  when it is not constrained by the data. If one treated the extraction of  $\rho_H(\omega)$  from  $C(\tau)$  as, e.g., a simple  $\chi^2$  minimization problem, one would have many flat directions in the parameter space. In maximum entropy method, one stabilizes the analysis by recasting it as a maximization of the combination

$$\mathcal{L} = -\frac{1}{2} \chi^2 + \alpha S, \quad (7a)$$

$$S = \sum_i \Delta\omega_i \left( \rho_H(\omega_i) - \rho_0(\omega_i) - \rho_H(\omega_i) \log \frac{\rho_H(\omega_i)}{\rho_0(\omega_i)} \right). \quad (7b)$$

Here  $\rho_0(\omega)$  is the default solution provided as an input to the analysis; in the absence of data, eq. (7) implies that  $\rho_H(\omega) = \rho_0(\omega)$ . Equation (7b) has the form of entropy in information theory, giving the method its name. Given a set of  $C(\tau)$ , the maximization of  $\mathcal{L}$ , eq. (7a) has a unique solution [10]. Note that this by itself does not guard against a solution unstable against noise. As pointed out by Bryan [11], parametrized suitably, the solution space can be restricted to the space spanned by singular directions [12] of the kernel in eq. (6a), whose dimensionality is no more than the number of data points.

While the early studies, refs [7–9], differed in some details, they found that the spectral function of  $J/\psi$  was not very sensitive to the phase transition: the changes in  $\rho_H(\omega)$  were small as one crossed  $T_c$ . A clear peak structure was found even at  $1.5T_c$ . In addition, the dissolution of the peak was found to be gradual rather than abrupt [7,8], with a broadening and weakening of the peak as one went to higher temperatures. On the other hand, the 1P states ( $\chi_c$ ) were seen to change much more abruptly across the transition. The spectral functions calculated in ref. [7] for the scalar,  $\bar{c}c$ , and vector,  $\bar{c}\gamma_5 c$ , operators are shown in figure 1a. The correlators  $c(\tau)$  show very little change in the vector channel as one crosses  $T_c$ , even upto  $1.5T_c$ ; this resulted in an extracted spectral function that showed a strong  $J/\psi$  peak even at  $1.5T_c$ . On the other hand,  $C(\tau)$  in the scalar channel showed serious modification on crossing  $T_c$ , and major weakening of the  $\chi_{c_0}$  peak was seen already at  $1.1T_c$ . Several follow-up studies reached qualitatively similar conclusions [13]. Also a dynamical study with 2-flavour QCD (but with a somewhat heavy pion) found very similar results, when temperatures are expressed in units of  $T_c$  [14]. A very recent dynamical study, again with a somewhat heavy pion, has also found very little change in the 1S state peaks upto temperatures  $\sim 1.4T_c$  [15].

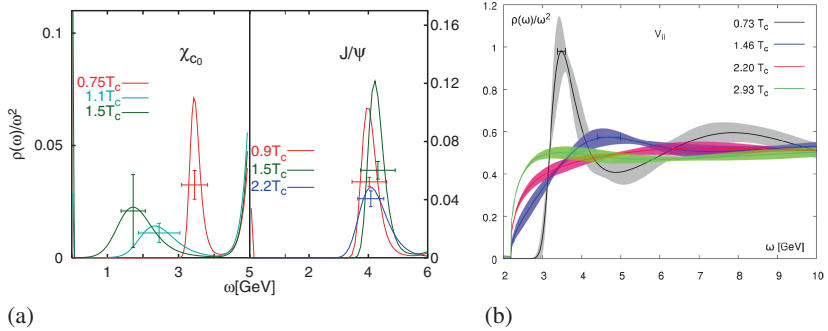


**Figure 1.** (a) Spectral functions of the  $\bar{c}c$  and  $\bar{c}\gamma_i c$  operators from ref. [7], showing the modification of  $\chi_{c_0}$  and survival of the  $J/\psi$  peak after deconfinement. The vertical error bar indicates the error for the reconstructed spectral function, averaged over the  $\omega$  range indicated by the horizontal band [10]. (b) Spectral function of the  $\bar{c}\gamma_i c$  operator ([19], ©American Physical Society) showing serious modification of the  $J/\psi$  peak already below  $1.5T_c$ . The band is the error estimate from a simple jack-knife analysis.

On the other hand, the systematics of the inversion of eq. (6) is large, and probably the extraction of  $\rho_H(\omega)$  is less reliable than what the convergence of the different results suggested. In particular, it was pointed out later that a large part of the change in the 1P channels is due to the diffusion peaks in these channels [16]. The free spectral function in the vector, axial vector, and scalar channels have a contribution

$$\rho_H(\omega) \xrightarrow{\omega \rightarrow 0} 2\pi \chi_H(T) \omega \delta(\omega), \quad (8)$$

which contribute an additive constant to  $C(\tau)$ . In the interacting theory, the  $\delta$  function becomes a smooth peak, leading to a near-constant term in the correlator. It has been shown [16,17] that much of the change in the 1P channel correlators comes from this low- $\omega$  contribution. It was also pointed out that even at small temperatures  $T \sim 0$ , when one restricts oneself to a small range in Euclidean time, it is difficult to isolate the peak structure from Euclidean correlator data [13]. In a series of papers, Mocsy and Petreczky [18] have shown that the lattice data of  $C(\tau)$  is also consistent with a large change in the peak structure at relatively smaller temperatures.

A recent study, similar in approach to refs [7,9] but using finer lattices [19], has found that even in the vector and pseudoscalar channels, the peak structure is considerably softened already at  $1.5T_c$ . Results from this study are also shown in figure 1b. It is to be understood that the analysis is similar to the earlier lattice studies, and can suffer from similar systematic effects. While it is certainly reasonable to hope that lattice QCD will be able to provide the spectral function with much better systematics in the future, it would be important to incorporate new ideas into the calculation.

In the bottomonia sector, there have been interesting recent studies [20,21] using the formalism of non-relativistic QCD (NRQCD) on the lattice [22]. Use of NRQCD has two advantages in this context. In NRQCD, the heavy quark mass  $m_Q$  is much larger than all other scales, and one replaces  $\omega$  in eq. (6b) by  $2M_Q + \omega$ . Then for  $M_Q \gg T$ , one replaces the periodic kernel eq. (6b) by a simple exponential,  $\exp(-\omega\tau)$ . Therefore, independent correlator data are now available for the whole range  $[0, \beta)$ . Also, as one is now studying

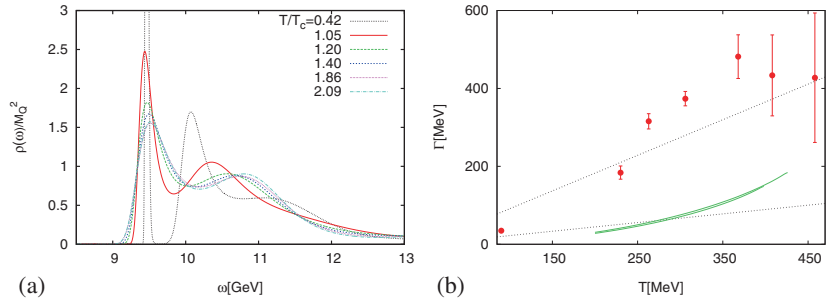


**Figure 2.** (a) Spectral function of the  $\bar{b}\gamma_{\mu}b$  current at various temperatures, extracted from lattice correlators [20]. A strong peak for  $\Upsilon(1S)$  survives even at  $\sim 2T_c$ . (b) Width of the  $\Upsilon(1S)$  peak at various temperatures, extracted from lattice correlators [20]. Also shown are (green, solid line) results of a calculation from HTL potential (see §2.2 and figure 3), and (black, dotted line) the trend from leading order of perturbation theory [20,24] for  $\alpha_s = 0.25$  (lower line) and 0.4 (upper line).

only excitations around  $2M_Q$ , the low- $\omega$  diffusion peak structure is absent. Aarts *et al* [20] calculated the correlators in this formalism, and applied Bayesian analysis, eq. (7), to extract  $\rho_H(\omega)$ . They found that 1S bottomonia survive at least till temperatures of  $2T_c$ ; see figure 2. On the other hand, the 1P peaks were found to dissolve right after  $T_c$  [21]. These results are qualitatively in agreement with the earlier, preliminary studies of bottomonia within the relativistic framework [23].

The peak position and the decay width of the 1S states have also been extracted from the NRQCD studies of the Euclidean correlator in ref. [20]. The decay width,  $\Gamma$ , calculated in ref. [20], is also shown in figure 2 (for their system,  $n_f = 2$  with  $m_q$  close to the strange quark mass,  $T_c$  is estimated to be  $\sim 220$  MeV). A near-linear increase of  $\Gamma$  with temperature is seen. It is interesting to note that in effective field theory calculations at weak coupling and  $\alpha_s m_Q \gg T$ ,  $\Gamma \sim 14 \alpha_s^3 T$  in leading order [20,24]. Within the rather large systematics, the lattice data are roughly in agreement with this for  $T \gtrsim 250$  MeV, for  $\alpha_s \sim 0.4$ . Note that figure 2 indicates a large decay width for the 1S bottomonia already above  $T_c$ . The origin of such a decay width would be collisions with the thermal quarks and gluons in the medium. Of course, the systematic error associated with the extraction of width from the Euclidean correlator is large, and Aarts *et al* [20] suggest that the calculated widths should be treated as an indicative upper limit. Preliminary results from another study, which also uses NRQCD formalism to calculate bottomonia correlators, have reported much smaller widths at comparable temperatures [25].

While lattice NRQCD provides a very promising method to study bottomonia in the medium, it is fair to say that the studies are still reasonably recent and various systematics need to be better examined.

## 2.2 Nonrelativistic approach and ‘potential at finite $T$ ’

A direct extraction of the spectral function from correlation functions calculated in lattice QCD is the most direct approach to understand the behaviour of quarkonia in deconfined plasma. Unfortunately, as discussed in the previous section, at the moment the systematics

of such a study are not in complete control. This is likely to change with time. However, it will surely help to supplement this direct approach with insights gained from other studies.

A nonrelativistic potential approach has been remarkably successful in quarkonia spectroscopy; it is therefore natural that several attempts have been made to extend such an approach to finite temperatures. The first step towards this was the identification of the free energy cost of putting an isolated  $Q\bar{Q}$  pair in a thermal medium [26]. As the distance between  $Q$  and  $\bar{Q}$  increases, in the confined medium the free energy cost of introducing such a pair also increases. As  $m_Q \rightarrow \infty$ , the quark is static and the effect of such a quark is approximated by a phase factor  $\sim e^{-m_Q\beta}$  multiplying a time-like gauge connection, called a Polyakov loop,  $L$ , defined as

$$P(x) = \prod_{i=0}^{N_\tau-1} U_0(\vec{x}, i) \quad (9a)$$

$$L(x) = \text{Tr } P(x). \quad (9b)$$

After suitable mass renormalizations, one can define the free energy cost mentioned above:

$$\mathcal{F}_{\text{QQ}}^{\text{av}}(\vec{x}) = \log\langle L(x)L^\dagger(0)\rangle. \quad (10)$$

Note that  $L(x)$  is invariant under colour rotations, and therefore, the free energy defined in eq. (10) includes an averaging over the colour orientations of  $Q$  and  $\bar{Q}$ . If one wants to study  $Q$  and  $\bar{Q}$  in a singlet combination, as in quarkonium, it can be defined using  $P(x)$ , eq. (9a) [27]:

$$\mathcal{F}_{\text{QQ}}^{\text{sing}}(\vec{x}) = \log\langle \text{Tr } P(x)P^\dagger(0)\rangle. \quad (11)$$

The right-hand side in the above equation is not gauge invariant, and therefore, needs to be calculated after fixing to a gauge. In perturbation theory, it can be shown that  $\mathcal{F}_{\text{QQ}}^{\text{sing}}(\vec{x})$  is gauge invariant, and in leading order, has the expression

$$\mathcal{F}_{\text{QQ}}^{\text{sing}}(\vec{x}) = -\frac{4}{3} \frac{\alpha_s}{r} e^{-m_D r}. \quad (12)$$

It has also been evaluated nonperturbatively, using eq. (11) in the Coulomb gauge [28].

$\mathcal{F}_{\text{QQ}}^{\text{sing}}(\vec{x})$  has been widely used in the literature to study the fate of quarkonia in QGP, by using it as a finite temperature potential; it denotes, though, a free energy, and not a potential. There has been considerable effort over the last decade towards constructing a suitable potential for quarkonia at finite temperature, in a field-theoretic framework [29–31]. In vacuum, the effective field theoretic framework for formally defining such a potential relies on the hierarchy of scales,  $m_Q \gg m_Q v \sim 1/r \gg E_b \sim m_Q v^2 \sim g^2/r$ , where  $v \ll 1$  is the relative velocity of the heavy quark,  $Q$ , and antiquark,  $\bar{Q}$ , in the bound state, and  $E_b$  is the binding energy. The idea is to write down an effective theory containing only the degrees of freedom relevant for  $\bar{Q}Q$  near the threshold, i.e., those at scale  $E_b$ . So scales of  $m_Q$  and  $m_Q v$  are integrated out. Integrating out of the scale  $m_Q$  leads to

standard nonrelativistic QCD (NRQCD), while further integrating out  $m_Q v$  leads to the so-called potential NRQCD (pNRQCD) [32], with Lagrangian

$$\begin{aligned} \mathcal{L}_{\text{pNRQCD}} = & S^\dagger(\vec{r}) \left( i\partial_0 - \frac{p^2}{2m_Q} - V_S(r) + \text{corr.} \right) S(\vec{r}) \\ & + O^\dagger(\vec{r}) \left( iD_0 - \frac{p^2}{2m_Q} - V_O(r) + \text{corr.} \right) O(\vec{r}) + \dots, \end{aligned} \quad (13)$$

where  $S$  and  $O$  denote  $\bar{Q}Q$  in singlet and octet representations, respectively, and  $V_{S,O}$  denote the corresponding potentials. The ... include the singlet–octet transition terms. For sufficiently heavy quarks such that  $m_Q v \gg \Lambda_{\text{QCD}}$ , the parameters of  $\mathcal{L}_{\text{pNRQCD}}$  can be obtained perturbatively.

At finite temperatures, a new set of scales related to the temperature  $T$  are introduced. At very high temperatures, one can write down a hierarchy  $T \gg m_D \sim gT \gg g^2 T$ , where  $m_D$  is the scale of screening of static charges and  $g^2 T$  is the inherently nonperturbative magnetic scale. Integrating out the scale  $T$  leads to the standard hard thermal loop (HTL) Lagrangian [33]. The form of the finite temperature potentials depend on the relative hierarchy of the thermal scales and the scales related to  $m_Q$  [30].

Let us take  $m_Q \gg T \gg m_Q v$ . Integrating out  $m_Q$  and  $T$  then leads to the HTL version of NRQCD. If  $m_Q v \sim m_D$ , integrating out these scales leads to a potential which was first derived in ref. [29] slightly differently. The spectral function relevant to the dilepton peak is connected to the Fourier transform of the real-time correlator

$$C^>(t, \vec{x}) = \int d^3x \langle J^\mu(t, \vec{x}) J_\mu(0, \vec{0}) \rangle, \quad (14)$$

where  $J^\mu(t, \vec{x})$  is the point vector current defined after eq. (2). Replacing  $J_\mu$  in eq. (14) by a point-split current

$$J_\mu^{\text{split}}(t, \vec{x}; \vec{r}) = \bar{\psi} \left( t, \vec{x} + \frac{\vec{r}}{2} \right) \gamma_\mu U \left( t; \vec{x} + \frac{\vec{r}}{2}, \vec{x} - \frac{\vec{r}}{2} \right) \psi \left( t, \vec{x} - \frac{\vec{r}}{2} \right), \quad (15)$$

it is easy to check that in the noninteracting theory for nonrelativistic quarks,  $C_{\text{split}}^>(t, \vec{x}; \vec{r})$  satisfies a Schrödinger-like equation

$$\left( i\partial_t - \left( 2m_Q - \frac{\nabla_r^2}{2m_Q} \right) \right) C_{\text{split}}^>(t, \vec{x}; \vec{r}) = 0 \quad (\text{to } \mathcal{O}(1/m_Q^2)). \quad (16)$$

In the interacting theory, one can define a potential by equating the left-hand side of eq. (16) to  $V(t, \vec{r}) C_{\text{split}}^>(t, \vec{x}; \vec{r})$ . Taking the static limit,  $m_Q \rightarrow \infty$ , one gets

$$i\partial_t W(\vec{r}, t) = V(\vec{r}, t) W(\vec{r}, t), \quad (17)$$

where  $W(\vec{r}, t)$  is the time-like Wilson loop. Going to the long time limit leads to

$$\begin{aligned} V(r) = & -\frac{4}{3}\alpha_s \left( \frac{e^{-m_D r}}{r} + m_D \right) - i\frac{8}{3}\alpha_s T \Phi(r) \\ \Phi(r) = & \int_0^\infty \frac{dz z}{(z^2 + 1)^2} \left( 1 - \frac{\sin zr}{zr} \right) \end{aligned} \quad (18)$$

in leading order HTL approximation [29,30].

While for the plasma formed in RHIC and LHC, the validity of the weak coupling approximation used in reaching eq. (18) is questionable, it is instructive to examine some features of the potential. The real part of  $V(r)$  is, modulo a constant, identical to the Debye-screened singlet free energy in eq. (12). Interestingly, there is also an imaginary part to the potential. The imaginary part leads to a thermal width  $\propto \alpha_s T$  of the spectral function peak, which incorporates the physics of Landau damping [34]. To get an idea of its contribution, ref. [29] treated the imaginary part as a perturbation, to get the decay width. For  $\Upsilon$  it was found that already at not-too-large temperatures  $\sim 250$  MeV, while the bound state survives, it acquires a considerable thermal width (see figure 3). This thermal width, though, is smaller than that extracted in ref. [20] from lattice correlators (see figure 2).

$V(r)$  (eq. (18)) was also used to calculate the spectral function, which is simply related to the Fourier transform of  $C^>(\vec{r} \rightarrow 0, t)$  [39]. It was found that for quarks in the bottom mass region, the spectral function peak is severely depleted and broadened already by  $T \sim 350$  MeV, and by a temperature of 450 MeV, no significant peak is visible (see figure 3). If one uses the potential for charmonium (where the separation of scales required is highly questionable), one finds that already at  $T \sim 250$  MeV, the peak structure is essentially absent. A similar study was also carried out in ref. [40], where various systematics were studied. The basic results are similar to ref. [39]. Also, the later study highlighted the major role played by the imaginary part of the potential in broadening the peak. Petreczky *et al* [40] also calculated the Euclidean correlators, and found that they do not completely agree with the bottomonia correlators obtained from the lattice.

As already mentioned, the hierarchy  $T \gg m_{QV}$  is not valid at the temperatures of interest in RHIC and LHC. At least for the  $\Upsilon$ , one in fact expects  $m_{QV} \gg T$ . In such a case, one first integrates out the scale  $m_{QV}$  from NRQCD, to get the pNRQCD action, eq. (13). Further integrating out the scale  $T$  then leads to thermal corrections which are very different from eq. (18) [30]. If  $m_D \gg E_b$ , the thermal potential is still well-defined, but the real part of the potential does not have the screened form. The potential still gets an imaginary component, which now has two main components: a term  $\propto \alpha_s^3 T$  which comes from a transition to colour-octet state, and terms like  $\alpha_s T m_D^2 r^2$  which are related to Landau damping. On the other hand, if  $E_b \gg m_D$ , the thermal potential is not well-

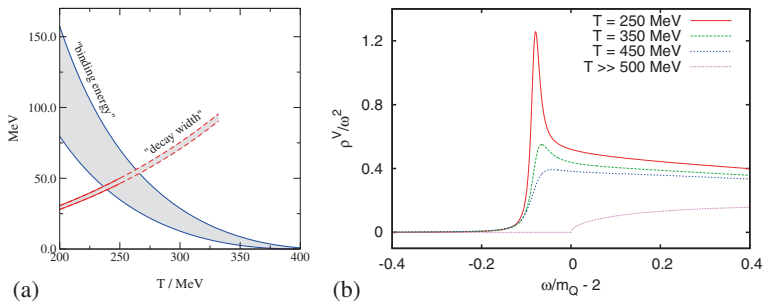


**Figure 3.** (a) Binding energy and decay width of the  $\Upsilon$  peak in the spectral function of the current  $\bar{b}\gamma b$ , using the leading-order HTL-resummed potential (from ref. [29]). (b) Spectral function calculated directly from the same potential [39]. Here  $m_Q = 4$  GeV.

defined. Of course, thermal corrections to the binding energy and decay width are well-defined quantities, and have been calculated in weak coupling [24]. The thermal decay width once again has contributions  $\propto \alpha_s^3 T$  related to singlet-to-octet transition, and terms  $\propto \alpha_s T m_D^2 r_0^2$  related to Landau damping [24], where  $r_0 = 3/(2\alpha_s m_Q)$  is the Bohr radius.

One message to take, from both the effective field theory studies and studies of the previous section, is that even before the dissolution of the quarkonia peak, the states can get a substantial thermal decay width. Rather than a single ‘dissolution temperature’, it is the temperature-dependent width which is of phenomenological significance. The decay width obtained from the imaginary part of the potential has been compared to phenomenological estimates of quarkonia dissociation in ref. [34].

In the discussion so far, we have stressed that the imaginary part of the ‘potential’ is a theoretical tool to describe the broadening of the quarkonium structure in the spectral function, due to interactions with the thermal gluons and quarks. Its interpretation has been further clarified using the language of open quantum systems [35,36]. Starting from a complete description of the  $\bar{Q}Q$  thermal medium, one can integrate out the thermal medium to get an effective description of the  $\bar{Q}Q$  system in the medium. Integrating out of the medium leads to noise terms in the description of the  $\bar{Q}Q$  system, which cause both dissipation of the heavy quark, and a lack of coherence between the  $\bar{Q}Q$  pair in quarkonia, leading to an increased thermal width. This has been worked out in perturbation theory, to give the same complex potential as above [36].

One can also try to calculate the potential, eq. (17), nonperturbatively, without assuming weak coupling or any particular ordering between the scales  $T$  and  $m_Q v$ . Burnier and Rothkopf [37] calculated the Euclidean time-like Wilson loop,  $W(\vec{r}, \tau)$ , and then employed an analytic continuation similar to that described in §2.1 to obtain the potential from it. A Bayesian analysis similar to, but not identical to, MEM was used [38], which probably needs careful examination. A complex potential was extracted from the Euclidean Wilson loop calculated in a gluon plasma. At  $2.33T_c$ , both the real and the imaginary parts of the potential extracted from the data are considerably different from the hard thermal loop calculation. Note that the time-like Wilson loop is identical to the Polyakov loop correlator in eq. (11), calculated in the axial gauge. Burnier and Rothkopf [37] also calculated the Polyakov loop correlator in Coulomb gauge. Analysing it in the same way, they obtained a potential which is much closer to the perturbative calculation of ref. [29]. Note that the Coulomb gauge calculation has already been done in great detail [28]; however it is not clear how sensitive the correlation function is to the imaginary part of the potential.

### 3. Prediction for quarkonia production in relativistic heavy-ion collision

In the previous section, we discussed various calculations that investigate the fate of a quarkonium put as a probe in static, equilibrated QGP. Of course, the experimental situation is very different. A  $c\bar{c}$  pair gets formed, probably in a hard collision at early times; the quarkonium state gets formed, either in the pre-equilibrium stage or in the plasma. Also the system is not static, the temperature profile changes. While understanding the

behaviour of an external  $J/\psi$  in static plasma is the first step to predict the  $J/\psi$  production in relativistic collisions, one needs to put it in the context of the fireball created in a heavy-ion collision. In this section we discuss some calculations towards quantitative prediction for  $J/\psi$  production in heavy-ion collision, and describe some ingredients for such a calculation.

### 3.1 ‘Regeneration’ and thermal quarkonia

The spirit of the discussion of §2 was that  $J/\psi$  is formed very early in the plasma, in a way possibly similar to that in a  $pp$  collision, and we investigate the survival probability of  $J/\psi$  in the QGP. The hadrons made of light quarks, on the other hand, are described very well by the assumption that as the medium cools to below deconfinement, the quarks present in the medium coalesce to form hadrons depending on a thermal distribution. If the density of  $c, \bar{c}$  is sufficiently high in the medium, one also needs to investigate the possibility that at freeze-out a  $c$  and a  $\bar{c}$  coalesce to form  $J/\psi$  [41]. In the literature, the production of  $J/\psi$  in this way is dubbed ‘regeneration’.

In regeneration calculations [41,42], the different hadrons with (open or hidden) charm are distributed statistically, just as the light hadrons are. The charm quarks are produced as  $\bar{c}c$  pairs in initial hard collisions, but then will develop in the plasma as coloured  $c(\bar{c})$  quarks. At the time of freeze-out, they then hadronize according to a statistical thermal distribution. So the ratios of, for example, different charmonia will follow a statistical distribution. An early motivation was the fact that the ratios of the production cross-section of  $\psi'$  and  $J/\psi$  in the 158 A GeV, Pb–Pb collisions in SPS followed a statistical distribution [41].

The number of  $J/\psi$  produced is given as

$$N_{J/\psi} = g_c^2 V n_{J/\psi}^{\text{th}}(T_{\text{fr}}, \mu_B), \quad (19)$$

where

$$n_i^{\text{th}} = g_i \int \frac{d^3 p}{e^{(E_i(p) - \mu_i)/T} \mp 1} \quad (20)$$

is the thermal (Bose/Fermi) distribution function for hadron  $i$ ,  $T_{\text{fr}}$  and  $\mu_B$  are the chemical freeze-out temperature and baryon chemical potential,  $V$  is the fireball volume, and  $g_c$  is an extra degeneracy factor to take into account the fact that the production of the charm quarks happen in hard collisions and the total number of charm quarks is much larger than it would have been if the charm quarks were chemically equilibrated in the plasma [41].

The model is simple, and is with clear predictions for rapidity and  $p_T$  distributions of  $J/\psi$ . The earlier works on this model [41] found good agreement of the relative yields of  $J/\psi$  and  $\psi'$  in the highest energy Pb–Pb runs of SPS. More recent studies [42] have also found good agreement of this ratio in RHIC. The early studies [41] had also predicted little or no suppression of  $J/\psi$  production in RHIC, and substantial enhancement in LHC, compared to scaled  $pp$  collision results. This has not been borne out by data. More detailed recent studies [42], which take into account the possibility that even in collisions that lead to a plasma in the core, there may be hard collisions between (surface) nuclei which do not lead to plasma formation, have reported good agreement with RHIC data for  $J/\psi$  production.

A generic prediction of the regeneration calculations is more suppression in the forward rapidity region than in midrapidity. This is in qualitative agreement with the trend seen in 200 A GeV, Au–Au collisions in RHIC. Also, as eq. (20) suggests, the  $p_T$  distribution will be rather steep. Assuming same  $T_{\text{fr}}$  as light hadrons, a much steeper  $p_T$  distribution is predicted than seen in the experiment [42]. A much larger freeze-out temperature  $\sim 360$  MeV, compared to the initial temperature, was required in ref. [42] to describe the  $p_T$  dependence in RHIC.

A variant of the regeneration mechanism has been suggested in ref. [43]. In their picture, while the initially produced  $\bar{c}c$  pair does not lead to  $J/\psi$  formation in the plasma, they do not become completely decorrelated. The motion of a heavy quark in plasma can be understood as a diffusion process [44,45], with a rather small diffusion coefficient [45,46]. The smallness of the diffusion coefficient, combined with the interaction between the  $\bar{c}c$  pair, lead to the  $c$  and  $\bar{c}$  staying spatially correlated through their evolution in the fireball. This, the authors argue, leads to a  $J/\psi$  cross-section larger than a naive regeneration calculation suggests, and a  $p_T$  distribution similar to that of the original  $\bar{c}c$  pair.

Some authors [47] have used a combination of directly produced and recombined  $J/\psi$  to explain the  $J/\psi$  yield, e.g., in RHIC. In [47], the  $J/\psi$  yield in SPS is almost completely directly produced. In RHIC, because of the hotter and larger fireball, a larger fraction of the directly produced  $J/\psi$  is suppressed, but some  $J/\psi$  are regenerated, giving a final suppression factor similar to SPS.

Another intuitive signature of regeneration would be the elliptic flow of  $J/\psi$  [48]. The charm quark shows substantial elliptic flow in RHIC [45]. If  $J/\psi$  is regenerated, it is expected to inherit this elliptic flow. On the other hand, a colour singlet  $J/\psi$  moving through the plasma will not show a substantial flow. While no significant elliptic flow of  $J/\psi$  was seen in RHIC, elliptic flow has been measured in LHC [49] and has been used to argue for substantial regeneration of  $J/\psi$  in the fireball created in LHC [50].

Due to the large mass of  $b$ , regeneration is usually considered to play a small role in the bottomonia sector. It has, however, been pointed out that the ratio of the different  $\Upsilon(nS)$  states can be explained by regeneration, assuming  $T_{\text{fr}} \sim 250$  MeV [51].

### 3.2 Quarkonia in the fireball

To calculate quarkonia production cross-section in the fireball produced in the relativistic heavy-ion collisions, e.g., the  $J/\psi$  or  $\Upsilon$  peak in dilepton channel, we need to incorporate the inputs from the previous sections in the framework of the evolution of the fireball. For using quarkonia as a marker of deconfinement, as originally envisaged by Matsui and Satz [1], one needs to have a theoretical calculation of quarkonia production for a given initial temperature of the plasma. For such a quantitative prediction, we need to have an understanding of the following processes:

- (a) The production of  $\bar{c}c$  pair, possibly in a hard  $gg$  collision.
- (b) Connecting the  $\bar{c}c$  pair to the  $J/\psi$  resonance.
- (c) Fate of  $J/\psi$  as it moves in the plasma, which is expanding and cooling.
- (d) Fate of other  $\bar{c}c$  resonances which can decay to  $J/\psi$ .
- (e) Possibility of generation of  $J/\psi$  at the freeze-out.

Usually the quarkonia yield in  $A$ – $A$  collisions is presented as  $R_{AA}$ , the ratio of the yield in  $A$ – $A$  collision to the scaled yield in  $pp$  collision (for the same window of variables like  $p_T$ ,  $y$  etc.):

$$R_{AA}(J/\psi) = \frac{N_{AA}(J/\psi)}{N_{\text{coll}} N_{pp}(J/\psi)}, \quad (21)$$

where  $N_{\text{coll}}$  is the number of binary collisions. A deviation of  $R_{AA}$  from 1 does not necessarily indicate medium effect. The production of  $\bar{c}c$  is a hard process; but the gluon distribution function is a nonperturbative input. These distribution functions can be different in the nucleus from that in the proton; e.g., the low  $x$  rise of the gluon distribution function can be tempered due to two low  $x$  gluons fusing ('shadowing'). Usually, one extracts the distribution functions in the nucleus from inputs like deep inelastic  $e$ – $A$  collisions as well as observables like dilepton and pion production in  $p$ – $A$  collisions [52].

The conversion of  $\bar{c}c$  to  $J/\psi$  is a complicated process even in vacuum [53]. Many calculations use the simple 'colour evaporation model', where production cross-section of  $J/\psi$  to the  $\bar{c}c$  production cross-section is given simply as

$$\sigma_{J/\psi}(s) \approx g_{\bar{c}c \rightarrow J/\psi} \sigma_{\bar{c}c}(s), \quad (22)$$

where  $g_{\bar{c}c \rightarrow J/\psi}$  is energy-independent [54]. Similar relations are written for other charmonia. A more rigorous approach is to use nonrelativistic QCD (NRQCD) [55]. One uses a separation of the scales  $m_Q$  and  $m_Q v$  to write down  $J/\psi$  as a superposition of a singlet  $\bar{c}c$  state and states where  $\bar{c}c$  are in an octet configuration, combining with  $g$  to form a colour singlet. The original  $\bar{c}c$  can form in either colour singlet or colour octet, and then evolves into  $J/\psi$  by emitting gluons. If we estimate the formation time of  $J/\psi$  as  $\tau_{J/\psi} \sim 1/E_b$ , the binding energy of the  $\bar{c}c$  pair, we get  $\tau_{J/\psi} \sim 0.5$  fm, which is of the order of the formation time of the plasma. For  $J/\psi$  with large  $p_T$ , time dilation increases the formation time further. So the in-medium behaviour of the precursor to  $J/\psi$  needs to be understood [56,57]. In particular, for large  $p_T$   $J/\psi$  the precursor is mostly in colour octet state, and it has been argued that it interacts much more readily with the medium, leading to dissolution [42,56] or quenching of  $p_T$  [57].

The interaction of  $J/\psi$  (and other quarkonia, which may decay into  $J/\psi$ ) with the medium is probably the most studied part of the scheme outlined above. Following the original intuitive argument of Matsui and Satz [1], many early works used a dissociation temperature, usually from using the singlet free energy in the Schrödinger equation. In a series of papers, Kharzeev and Satz studied the dissociation of  $J/\psi$  (and its precursor, the colour octet state) through gluon dissociation, generalizing the multipole analysis [58] for thermal gluons. For thermal gluons, a free gluon gas distribution has been used, which is probably not a good approximation at temperatures of interest to RHIC and LHC. A similar approach has been followed in ref. [57].

Ideally, the temperature modification of  $J/\psi$  and  $\Upsilon$  should be incorporated by putting in the corresponding spectral function. However, that is more difficult; what has been done in refs [59,60] is to use the imaginary part of the potential to calculate a thermal decay width, and evolve that through the history of the plasma to calculate a suppression factor  $R_{AA}$ . On the other hand, in ref. [61] the decay width is obtained from the imaginary part of the quark propagator, which incorporates the scattering T matrix, which can be evaluated self-consistently through a Bethe–Salpeter equation [62]. The  $QQ$  potential is an input in the Bethe–Salpeter equation.

It is worth mentioning here that in many studies, the real part of the potential is replaced by an ‘internal energy’ [63], which is obtained by subtracting an entropy term from the singlet free energy, eq. (11). This has largely been motivated by the fact that use of the free energy seems to give too large a suppression for both  $J/\psi$  and  $\Upsilon(1S)$ . As the discussion in §2.2 shows, however, there is little theoretical justification for using such an ‘internal energy’ for study of quarkonia dissociation in plasma.

In order to quantitatively study the  $J/\psi$  peak, it is not enough to study the modification of  $J/\psi$  in the plasma. Almost half of  $J/\psi$  seen in a  $pp$  collision come from a ‘feed-down’ route: the original  $\bar{c}c$  pair goes to  $\chi$  and  $\psi(2s)$  states, which have a substantial branching fraction to  $J/\psi$ . Some  $J/\psi$  also come from decays of the  $B$  mesons: at Tevatron, this fraction has been estimated to be  $\sim 9 \pm 1\%$  [64]. The time-scale for the  $B \rightarrow J/\psi$  decay is  $ps$ , and  $J/\psi$  coming from  $B$  can be subtracted out; the  $J/\psi$  yield after such a subtraction is referred to as ‘prompt’  $J/\psi$  [64,65]. Time-scales for the feed-down decays from  $\chi_c$  and  $\psi'$  are  $\sim 200$  fm or more. So these states are expected to move through the medium as the excited states. The fraction of  $J/\psi$  coming from  $\psi'$  and  $\chi_c$  states have been estimated to be  $\sim 9 \pm 3\%$  and  $\sim 30 \pm 7\%$  at Tevatron, and similar values at lower energies [66]. For  $\Upsilon(1S)$ , the CDF Collaboration has measured the feed-down fraction in Tevatron [67]: for  $p_T > 8$  GeV, the fraction of directly produced  $\Upsilon(1S)$  is about  $51 \pm 12\%$ , while about  $11 \pm 8\%$  come from the decay of excited  $\Upsilon$  and  $38 \pm 9\%$  come from  $\chi_b$  decays. As the excited  $\chi$  or  $\psi'$  states are more readily dissolved by the medium [2,3,7,56], about 50% suppression of the  $J/\psi$  and  $\Upsilon(1S)$  yield can come simply from the melting of the excited states in medium into open charm.

#### 4. Experimental results

There has been an immense body of experimental results on  $J/\psi$  and  $\Upsilon$ , starting from the early experimental efforts to create quark-gluon plasma. For completeness, we mention some trends from the experiments; detailed survey of the experimental results can be found elsewhere [68,69].

$J/\psi$  suppression compared to  $pp$  collisions was already seen at the O–Cu and S–U collisions in the NA38/NA50 experiments in SPS, CERN. However, this suppression could be completely understood in terms of cold nuclear matter effect, like shadowing (§3.2) and interaction of  $J/\psi$  with nuclear matter, taking a nuclear absorption cross-section  $\sigma_{J/\psi N}^{\text{abs}} \approx 4$  mb and  $\sigma_{\psi' N}^{\text{abs}} \approx 7$  mb [70]. The investigation of cold nuclear matter effects can be done by conducting  $p$ – $A$  collisions at the same energy. This has now become a staple of the experimental programme, and understanding the quarkonia yield in such collisions is vital before one can interpret the suppression in  $A$ – $A$  collisions.

A larger suppression of  $J/\psi$  than what can be explained by cold nuclear matter effects was observed by the NA50 experiment in 158 A GeV Pb–Pb collisions in SPS. This suggested an onset of deconfinement [4]. A large suppression has also been seen in the 200 A GeV Au–Au collisions in RHIC (figure 4). The level of suppression seen was somewhat similar to that seen in SPS, which was a surprise, given the much larger centre-of-mass energy and the expectation of a much longer living plasma. One way to explain the data was to assume that in both experiments the plasma was hot enough to dissolve the excited  $\chi_c$  and  $\psi'$  states, but not hot enough to melt the directly produced  $J/\psi$  [71]. The data could also be explained in other ways: e.g. it is possible that a larger part of the directly

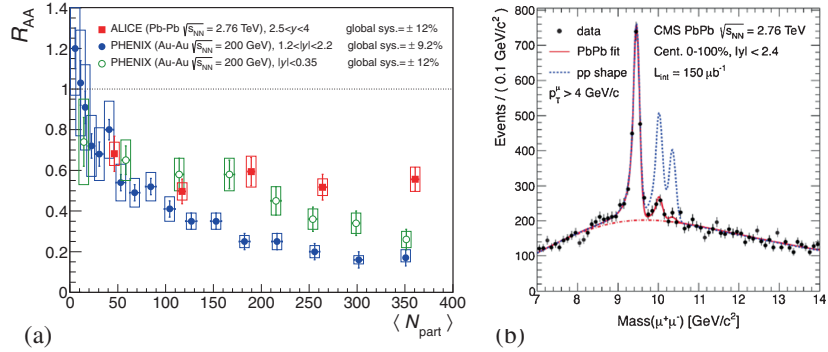


**Figure 4.** (a)  $J/\psi$   $R_{AA}$  measured by the ALICE experiment in the Pb–Pb collisions in LHC at 2.76 A TeV, compared to 200 A GeV Au–Au results from PHENIX ([75], ©American Physical Society). (b)  $\Upsilon$  peaks in the dimuon channel at midrapidity, from CMS [69,80]. The  $\Upsilon(1S)$  peak has been normalized to the  $pp$  collision, showing the suppression of the  $\Upsilon(2S)$  and  $\Upsilon(3S)$  states.

produced  $J/\psi$  was dissolved in the RHIC experiment, but there was some  $J/\psi$  produced via recombination (§3.1), to keep the total yield similar [72]. Other attempts to explain the total yield have used only regeneration [42]. As explained in §3.1, regeneration calculations have been fairly successful in describing the rapidity dependence of the  $J/\psi$  suppression, but have had difficulty in explaining the  $p_T$  dependence [73,74].

The data from the Pb–Pb collisions at much larger centre-of-mass energy (2.76 A TeV) (but in the forward rapidity region), as measured by the ALICE Collaboration [75], are also shown in figure 4. The data do not show a much stronger suppression. Data at midrapidity, but larger  $p_T$ , from CMS [65] show suppression at levels similar to the PHENIX data in figure 4. A combination of suppression and recombination has been suggested to explain the data [76]. However, details of the  $p$ –Pb data for charmonia have not been completely understood [68,77].

An interesting suggestion has been to look not at the  $R_{AA}$  but the ratio of  $J/\psi$  with open charm cross-section [78,79]. This will remove the uncertainties due to the nuclear distribution functions. The double ratio [79]

$$S_{J/\psi} = \frac{g_{\bar{c}c \rightarrow J/\psi}^{AA}}{g_{\bar{c}c \rightarrow J/\psi}^{PP}}, \quad g_{\bar{c}c \rightarrow J/\psi} = \frac{N(J/\psi)}{N(\bar{c}c)} \quad (23)$$

then shows the medium modification of  $J/\psi$  binding. Using this quantity, Satz has claimed that the forward rapidity/large  $p_T$  data of LHC does not show any anomalous suppression of  $J/\psi$ , while the RHIC data in figure 4 do [79].

A very beautiful measurement of the  $\Upsilon$  production from the CMS experiment avoids many of the experimental uncertainties, and offers a way of studying  $\Upsilon$  suppression in the Pb–Pb collisions in LHC. Figure 4b shows the  $\Upsilon$  peaks in the dimuon channel, where the  $\Upsilon(1S)$  peak has been normalized to agree with the peak in  $pp$  collisions. Then the peaks for  $\Upsilon(2S)$  and  $\Upsilon(3S)$  are considerably suppressed. In fact, the  $R_{AA}$  value for  $\Upsilon(1S)$  is quoted as  $0.56 \pm 0.08 \pm 0.07$  [80]. From the discussion at the end of §3.2,

this is consistent with no suppression of direct  $\Upsilon(1S)$  but almost complete suppression of the feeddown component. This is in line with what one would expect if, following the lattice studies, one expects  $\Upsilon(1S)$  not to be modified much in the plasma at moderate temperatures, while the excited states melt readily (§2.1). Note, however, that the large decay widths shown in figure 2 would suggest a substantial suppression of  $\Upsilon(1S)$  also.  $R_{AA}$  for  $\Upsilon(2S)$  is  $0.12 \pm 0.04 \pm 0.02$  and that for  $\Upsilon(3S)$  is  $< 0.1$  [80], indicating major dissociation of these states.

## 5. Summary and outlook

In this article, the current status of our understanding of quarkonia yield in relativistic heavy-ion collisions is presented. Conceptually, a lot of insight has been gained in the last decade, and the simple picture of quarkonia dissociation due to Debye screening has been replaced by a detailed understanding of the dissociation mechanism from QCD.

Lattice QCD (§2.1) has emerged as a pre-eminent tool for understanding the behaviour of quarkonia in static plasma. But getting quantitative information about the spectral function, decay width etc. have so far been difficult. While it is likely that eventually we shall be able to extract the physics from lattice correlators, it probably will require some new ideas. One recent idea has been nonrelativistic QCD on lattice, which is a very promising tool for bottomonia at least. Simultaneously, other approaches, largely based on perturbative NRQCD, have clarified many misconceptions (§2.2). One development has been a theoretically justified construction of a finite temperature effective potential, and illustration of how it captures effects like thermal gluon dissociation.

The calculation of quarkonia yield in the expanding fireball produced in heavy-ion collisions is more challenging. In §3.2 necessary steps are discussed, and some calculations that try to incorporate many of the formal developments of §2.1 in them are outlined. Of course, for such a calculation one needs to know the behaviour of a quarkonium moving with respect to the medium. Some preliminary calculations exist in that direction [81], but clearly more needs to be done. Some other major uncertainties pertain to the formation of  $J/\psi$ , and interaction of the medium with the precursor to the  $J/\psi$ .

Almost three decades after the suggestion of quarkonia as a probe of the deconfined medium, it remains a topic of great interest. While still not as a thermometer of the plasma as originally envisaged by Satz and others [2], it has been an invaluable source of insight into the nature of the deconfined medium.

## Acknowledgements

The author would like to thank Mikko Laine and Jon-Ivar Skullerud for providing him with data related to figures 2 and 3. The first draft of this article was completed during WHEPP-13. The author also acknowledges discussions with the participants of the meeting, in particular with D Das, S Gupta, R Gavai, R Sharma, P Shukla and K Sridhar.

## References

- [1] T Matsui and H Satz, *Phys. Lett. B* **178**, 416 (1986)
- [2] F Karsch, M T Mehr and H Satz, *Z. Phys. C* **37**, 617 (1988)

- [3] S Digal, P Petreczky and H Satz, *Phys. Rev. D* **64**, 094015 (2001),
- [3a] Throughout this report, we shall be discussing nucleus–nucleus collisions, with a given energy per nucleon. In such cases, the energy will be written as xxx A GeV, where xxx GeV is the energy per nucleon and A is the mass number
- [4] NA50 Collaboration: M C Abreu *et al*, *Phys. Lett. B* **477**, 28 (2000)
- [5] M Le Bellac, *Thermal field theory* (Cambridge University Press, 1996)
- [6] O Philipsen, *Prog. Part. Nucl. Phys.* **70**, 55 (2013);  
P Petreczky, *J. Phys. G* **39**, 093002 (2012)
- [7] S Datta, F Karsch, P Petreczky and I Wetzorke, *Nucl. Phys. Proc. Suppl.* **119**, 487 (2003);  
*Phys. Rev. D* **69**, 094507 (2004)
- [8] K Nomura, O Miyamura, T Umeda and H Matsufuru, *Nucl. Phys. Proc. Suppl.* **119**, 496 (2003)  
T Umeda, H Matsufuru and K Nomura, *Eur. Phys. J. C* **39S1**, 9 (2005)
- [9] M Asakawa and T Hatsuda, *Phys. Rev. Lett.* **92**, 012001 (2004)
- [10] M Jarrell and J E Gubernatis, *Phys. Rep.* **269**, 133 (1996)  
M Asakawa and T Hatsuda, *Prog. Part. Nucl. Phys.* **46**, 459 (2001)
- [11] R K Bryan, *Eur. Biophys. J.* **18**, 165 (1990)
- [12] W Press, S Teukolsky, W Vetterling and B Flannery, *Numerical recipes* (Cambridge University Press, 1989)
- [13] A Jakovac, P Petreczky, K Petrov and A Velytsky, *Phys. Rev. D* **75**, 014506 (2007)
- [14] G Aarts *et al*, *Phys. Rev. D* **76**, 094513 (2007)  
M Oktay and J-I Skullerud, arXiv:1005.1209
- [15] S Borsanyi *et al*, *J. High Energy Phys.* **1404**, 132 (2014)
- [16] T Umeda, *Phys. Rev. D* **75**, 094502 (2007)
- [17] S Datta and P Petreczky, *J. Phys. G* **35**, 104114 (2008)  
P Petreczky, *Eur. Phys. J. C* **62**, 85 (2009)
- [18] A Mocsy and P Petreczky, *Eur. Phys. J. ST* **155**, 101 (2008); *Phys. Rev. Lett.* **99**, 211602 (2007)
- [19] H T Ding *et al*, *Phys. Rev. D* **86**, 014509 (2012)
- [20] G Aarts *et al*, *J. High Energy Phys.* **1111**, 103 (2011)
- [21] G Aarts *et al*, *J. High Energy Phys.* **1312**, 064 (2013)
- [22] G P Lepage *et al*, *Phys. Rev. D* **46**, 4052 (1992)
- [23] S Datta, A Jakovac, F Karsch and P Petreczky, *AIP Conf. Proc.* **842**, 35 (2006)
- [24] N Brambilla, M Escobedo, J Ghiglieri, J Soto and A Vairo, *J. High Energy Phys.* **1009**, 038 (2010)
- [25] S Kim, P Petreczky and A Rothkopf, *PoS Lattice* **2013**, 169 (2014)
- [26] L McLerran and B Svetitsky, *Phys. Rev. D* **24**, 450 (1981)
- [27] S Nadkarni, *Phys. Rev. D* **34**, 3904 (1986)
- [28] O Kaczmarek, F Karsch, P Petreczky and F Zantow, *Phys. Lett. B* **543**, 41 (2002)  
O Kaczmarek and F Zantow, *Phys. Rev. D* **71**, 114510 (2005)
- [29] M Laine, O Philipsen, P Romatschke and M Tassler, *J. High Energy Phys.* **0703**, 054 (2007)
- [30] N Brambilla, J Ghiglieri, A Vairo and P Petreczky, *Phys. Rev. D* **78**, 014017 (2008)
- [31] A Beraudo, J-P Blaizot and C Ratti, *Nucl. Phys. A* **806**, 312 (2008)
- [32] For a review, see N Brambilla, A Pineda, J Soto and A Vairo, *Rev. Mod. Phys.* **77**, 1423 (2005)
- [33] R D Pisarski, *Phys. Rev. Lett.* **63**, 1129 (1989)
- [34] N Brambilla, M Escobedo, J Ghiglieri and A Vairo, *J. High Energy Phys.* **1112**, 116 (2011)
- [35] C Young and K Dusling, *Phys. Rev. C* **87**, 065206 (2013)  
N Borghini and C Gombeaud, *Eur. Phys. J. C* **72**, 2000 (2012)  
Y Akamatsu and A Rothkopf, *Phys. Rev. D* **85**, 105011 (2012)
- [36] Y Akamatsu, *Phys. Rev. D* **87**, 045016 (2013)
- [37] Y Burnier and A Rothkopf, *Phys. Rev. D* **87**, 114019 (2013)

- [38] Y Burnier and A Rothkopf, *Phys. Rev. Lett.* **111**, 182003 (2013)
- [39] Y Burnier, M Laine and M Vepsalainen, *J. High Energy Phys.* **0801**, 043 (2008)
- [40] P Petreczky, C Miao and A Mocsy, *Nucl. Phys. A* **855**, 125 (2011)
- [41] P Braun-Munzinger and J Stachel, *Phys. Lett. B* **490**, 196 (2000)  
R L Thews, M Schroedter and J Rafelski, *Phys. Rev. C* **63**, 054905 (2001)
- [42] A Andronic, P Braun-Munzinger, K Redlich and J Stachel, *Nucl. Phys. A* **789**, 334 (2007)
- [43] C Young and E Shuryak, *Phys. Rev. C* **79**, 034907 (2009)
- [44] G D Moore and D Teaney, *Phys. Rev. C* **71**, 064904 (2005)
- [45] PHENIX Collaboration: A Adare *et al*, *Phys. Rev. C* **84**, 044905 (2011)
- [46] A Francis, O Kaczmarek, M Laine and J Langelage, *PoS Lattice* **2011**, 202 (2011)  
D Banerjee, S Datta, R Gavai and P Majumdar, *Phys. Rev. D* **85**, 014510 (2012)
- [47] L Grandchamp and R Rapp, *Nucl. Phys. A* **715**, 545 (2003)
- [48] L Yan, P Zhuang and N Xu, *Phys. Rev. Lett.* **97**, 232301 (2006)
- [49] ALICE Collaboration: E Abbas *et al*, *Phys. Rev. Lett.* **111**, 162301 (2013)
- [50] X Zhao, A Emerick and R Rapp, *Nucl. Phys. A* **904–905**, 611c (2013)
- [51] S Gupta and R Sharma, *Phys. Rev. C* **89**, 057901 (2014)
- [52] See K J Eskola, H Paukkunena and C A Salgado, *J. High Energy Phys.* **0904**, 065 (2009), for a recent estimate of the nuclear distribution functions
- [53] Quarkonium Working Group: N Brambilla *et al*, *Heavy quarkonium physics*, CERN Report (hep-ph/0412158)
- [54] R Gavai *et al*, *Int. J. Mod. Phys. A* **10**, 3043 (1995)
- [55] G T Bodwin, E Braaten and G P Lepage, *Phys. Rev. D* **51**, 1125 (1995)
- [56] D Kharzeev and H Satz, *Phys. Lett. B* **334**, 155 (1994)  
X Xu, D Kharzeev, H Satz and X Wang, *Phys. Rev. C* **53**, 3051 (1996)
- [57] R Sharma and I Vitev, *Phys. Rev. C* **87**, 044905 (2013)
- [58] G Bhanot and M Peskin, *Nucl. Phys. B* **156**, 391 (1979)
- [59] M Strickland and D Bazow, *Nucl. Phys. A* **879**, 25 (2012)
- [60] M Margotta *et al*, *Phys. Rev. D* **83**, 105019 (2011)
- [61] F Riek and R Rapp, *New J. Phys.* **13**, 045007 (2011)
- [62] M Mannarelli and R Rapp, *Phys. Rev. C* **72**, 064905 (2005)  
D Cabrera and R Rapp, *Phys. Rev. D* **76**, 114506 (2007)
- [63] O Kaczmarek, F Karsch, P Petreczky and F Zantow, *Nucl. Phys. Proc. Suppl.* **129**, 560 (2004)  
O Kaczmarek and F Zantow, *Eur. Phys. J. C* **43**, 59 (2005)
- [64] CDF Collaboration: D Acosta *et al*, *Phys. Rev. D* **71**, 032001 (2005)
- [65] CMS Collaboration: S Chatrchyan *et al*, *J. High Energy Phys.* **05**, 063 (2012)
- [66] P Faccioli, C Lourenco, J Seixas and H Woehri, *J. High Energy Phys.* **0810**, 004 (2008)  
CDF Collaboration: F Abe *et al*, *Phys. Rev. Lett.* **79**, 578 (2003)
- [67] T Affolder *et al*, *Phys. Rev. Lett.* **84**, 2094 (2000)
- [68] D Das, *Conf. Proc.* **57**, 37–44 (2012) (*Proceedings of the DAE Symposium on Nuclear Physics*, 2012, arXiv:1212.2704)  
A Rossi, EPJ Web Conf. **60**, 03003 (2013) (*Proceedings of the LHCP Conference*, arXiv:1308.2973)
- [69] I Tserruya, *Proceedings of the New Trends in High Energy Physics*; arXiv:1311.4456
- [70] NA50 Collaboration: B Alessandro *et al*, *Phys. Lett. B* **553**, 167 (2003); *Eur. Phys. J. C* **33**, 31 (2004)
- [71] F Karsch, D Kharzeev and H Satz, *Phys. Lett. B* **637**, 76 (2006)
- [72] X Zhao and R Rapp, *Phys. Lett. B* **664**, 253 (2008)
- [73] PHENIX Collaboration: A Adare *et al*, *Phys. Rev. Lett.* **98**, 232301 (2007)
- [74] PHENIX Collaboration: A Adare *et al*, *Phys. Rev. C* **84**, 054912 (2011)
- [75] ALICE Collaboration: B Abelev *et al*, *Phys. Rev. Lett.* **109**, 072301 (2012)

*Quarkonia in heavy-ion collisions*

- [76] X Zhao and R Rapp, *Nucl. Phys. A* **859**, 114 (2011)
- [77] ALICE Collaboration: B Abelev *et al*, *J. High Energy Phys.* **1402**, 073 (2014)  
L Manceau, EPJ Web Conf. **60**, 13002 (2013), *Proceedings of the LHCP Conference*;  
arXiv:1307.3098
- [78] K Sridhar and H Satz, *Phys. Rev. D* **50**, 3557 (1994)
- [79] H Satz, *Adv. High Energy Phys.* **2013**, 242918 (2013)
- [80] S Chatrchyan *et al*, *Phys. Rev. Lett.* **109**, 222301 (2012)
- [81] S Datta *et al*, in: *Proceedings of the Strong and Electroweak Matter 2004* (Helsinki, Finland),  
arXiv:hep-lat/0409107.  
G Aarts *et al*, *Nucl. Phys. A* **785**, 1c (2007), *Proceedings of the Strong and Electroweak Matter  
2006* (Brookhaven, USA)  
S Kim *et al*, *PoS Lattice* **2012**, 086 (2012)